# Hypoxia induces a glycolytic complex in intestinal epithelial cells independent of HIF-1-driven glycolytic gene expression

Kierans, Sarah J; Fagundes, Raphael R; Malkov, Mykyta I; Sparkes, Ríona; Dillon, Eugène T; Smolenski, Albert; Faber, Klaas Nico; Taylor, Cormac T

*Published in:*
Proceedings of the National Academy of Sciences of the United States of America

*DOI:*
10.1073/pnas.2208117120

PNAS RESEARCH ARTICLE | CELL BIOLOGY

# Hypoxia induces a glycolytic complex in intestinal epithelial cells independent of HIF-1-driven glycolytic gene expression

Sarah J. Kierans[a,b], Raphael R. Fagundes[c], Mykyta I. Malkov[a,b], Ríona Sparkes[a,b], Eugène T. Dillon[b], Albert Smolenski[a,b], Klaas Nico Faber[c], and Cormac T. Taylor[a,b,d,1]

Edited by Matthew Vander Heiden, Koch Institute at Massachusetts Institute of Technology, Cambridge, Massachusetts, United States; received May 30, 2022; accepted July 11, 2023 by Editorial Board Member Barbara B. Kahn

**The metabolic adaptation of eukaryotic cells to hypoxia involves increasing dependence upon glycolytic adenosine triphosphate (ATP) production, an event with consequences for cellular bioenergetics and cell fate. This response is regulated at the transcriptional level by the hypoxia-inducible factor-1(HIF-1)-dependent transcriptional upregulation of glycolytic enzymes (GEs) and glucose transporters. However, this transcriptional upregulation alone is unlikely to account fully for the levels of glycolytic ATP produced during hypoxia. Here, we investigated additional mechanisms regulating glycolysis in hypoxia. We observed that intestinal epithelial cells treated with inhibitors of transcription or translation and human platelets (which lack nuclei and the capacity for canonical transcriptional activity) maintained the capacity for hypoxia-induced glycolysis, a finding which suggests the involvement of a nontranscriptional component to the hypoxia-induced metabolic switch to a highly glycolytic phenotype. In our investigations into potential nontranscriptional mechanisms for glycolytic induction, we identified a hypoxia-sensitive formation of complexes comprising GEs and glucose transporters in intestinal epithelial cells. Surprisingly, the formation of such glycolytic complexes occurs independent of HIF-1-driven transcription. Finally, we provide evidence for the presence of HIF-1α in cytosolic fractions of hypoxic cells which physically interacts with the glucose transporter GLUT1 and the GEs in a hypoxia-sensitive manner. In conclusion, we provide insights into the nontranscriptional regulation of hypoxia-induced glycolysis in intestinal epithelial cells.**

HIF | hypoxia | glycolysis | metabolism

## Significance

In hypoxia, cells undergo a metabolic switch toward an enhanced rate of glycolysis. This has important implications for cell behavior, phenotype, and fate in both cancerous and healthy cells. Here, we describe a mechanism by which hypoxia, in addition to increasing glycolytic enzyme expression via HIF-1α (hypoxia-inducible factor-1α), promotes glycolysis via the nontranscriptional formation of a metabolic complex in human intestinal epithelial cells.

Under hypoxic conditions, eukaryotic cells have evolved the capacity to alter their metabolic strategy to maintain adenosine triphosphate (ATP) production through increased flux through the glycolytic pathway when oxygen ($O_2$) and, consequently, mitochondrial respiration become limited (1). This metabolic switch to a highly glycolytic phenotype is now recognized to not only contribute to bioenergetic homeostasis and cell survival but also underpins important changes in both the phenotype and function of rapidly dividing cells such as proliferating immune, endothelial, and tumor cells (2–4). Understanding the fundamental mechanism(s) unpinning the regulation of glycolysis in response to hypoxia is therefore of key importance for understanding the cellular physiology and pathophysiology of an array of biological processes and diseases. However, our understanding of the complete mechanisms underpinning the regulation of glycolysis, particularly during periods of metabolic stress such as hypoxia, remains limited.

Following a hypoxic insult, enhanced flux through the glycolytic pathway is initiated by a reduction in ATP and consequent reduction in the allosteric inhibition of ATP on glycolytic enzymes (GEs) phosphofructokinase and pyruvate kinase to promote flux through the pathway (5). This allosteric regulation of glycolysis is subsequently followed by a hypoxia-dependent transcriptional upregulation of genes encoding glucose transporters (e.g., GLUT1) and all 10 GEs, a response mediated by the hypoxia-inducible factor-1 (formed by the dimerization of HIF-1α and HIF-1β) (1). Thirdly, and more controversially, glycolysis has been described to be enhanced via the formation of a glycolytic metabolon (6, 7); a physical metastructure composed of multiple glycolytic and functionally associated proteins in plants (*Arabidopsis thaliana*) (8, 9), yeast (*Saccharomyces cerevisiae*) (10, 11), protists (*Trypanosoma brucei*) (12, 13), and nematodes (*Caenorhabditis elegans*) (14). In these organisms, the compartmentalization of glycolysis is beneficial for intracellular kinetics as flux through the glycolytic pathway is enhanced by channeling of substrates between sequential pathway enzymes which minimizes the need for a rapid equilibration of substrate levels across the entire cytosol. However, while such complexes have been well characterized in other species, many questions remain with respect to glycolytic complexes in mammalian cells. Although evidence supports the existence of these interactions in mammalian cells

Author affiliations: [a]University College Dublin School of Medicine, University College Dublin, Dublin D4, Ireland; [b]Conway Institute of Biomolecular and Biomedical Research, University College Dublin, Dublin D4, Ireland; [c]Department of Gastroenterology and Hepatology, University Medical Center Groningen, University of Groningen, Groningen D4, The Netherlands; and [d]Systems Biology Ireland, University College Dublin, Dublin D4, Ireland

Author contributions: S.J.K. and C.T.T. designed research; S.J.K., R.R.F., M.I.M., R.S., E.T.D., and A.S. performed research; R.R.F., A.S., and K.N.F. contributed new reagents/analytic tools; S.J.K. and E.T.D. analyzed data; and S.J.K. and C.T.T. wrote the paper.

The authors declare no competing interest.

This article is a PNAS Direct Submission. M.V.H. is a guest editor invited by the Editorial Board.



[1]To whom correspondence may be addressed. Email: cormac.taylor@ucd.ie.

This article contains supporting information online at https://www.pnas.org/lookup/suppl/doi:10.1073/pnas.2208117120/-/DCSupplemental.

Published August 21, 2023.

(15–21), our understanding of the importance of these complexes during periods of metabolic stress such as hypoxia requires further investigation.

In this study, we hypothesised that hypoxia not only enhances glycolysis through the HIF-1-dependent increase of GE expression, but also by additional nontranscriptional mechanisms. The nontranscriptional mechanism indentified here involves the formation of a glycolytic complex which may facilitate glucose metabolism and support cellular metabolic adaptation to hypoxic stress.

## Results

**Hypoxia-Induced Glycolysis Occurs in Intestinal Epithelial Cells Where De Novo Gene Transcription and Translation are Inhibited.** We first investigated the impact of hypoxia (1% $O_2$) on the induction of glycolysis in Caco-2 cells. The perception of hypoxia by Caco-2 cells was demonstrated by a hypoxia-sensitive, time-dependent stabilization of HIF-1α (Fig. 1*A*) and transcriptional upregulation of HIF-1-dependent genes which encode proteins central to glucose metabolism including glucose transporter GLUT1 and lactate producing enzyme, lactate dehydrogenase-A (LDHA) (Fig. 1*B*). Glycolytic activity in these cells was determined by measuring end point extracellular lactate accumulation (Lactate$_e$; Fig. 1*C*) as a marker of glycolytic metabolism. Caco-2 cells demonstrated a time-dependent and hypoxia-sensitive increase in glycolysis when compared to normoxic controls, highlighting the responsiveness of these cells to hypoxia.

Given that the primary regulatory mechanism for hypoxia-induced glycolysis occurs at a transcriptional level through the HIF-1-dependent transcriptional upregulation of GEs and glucose transporters, we next investigated the impact of inhibiting de novo gene transcription and protein translation on hypoxia-induced glycolysis. Hypoxia induced an enhanced level of glycolysis in Caco-2 cells compared to normoxic controls even when de novo gene transcription (Fig. 1*D*) or protein translation (Fig. 1*E*) was inhibited using actinomycin D (ACND) or cycloheximide (CHX) respectively

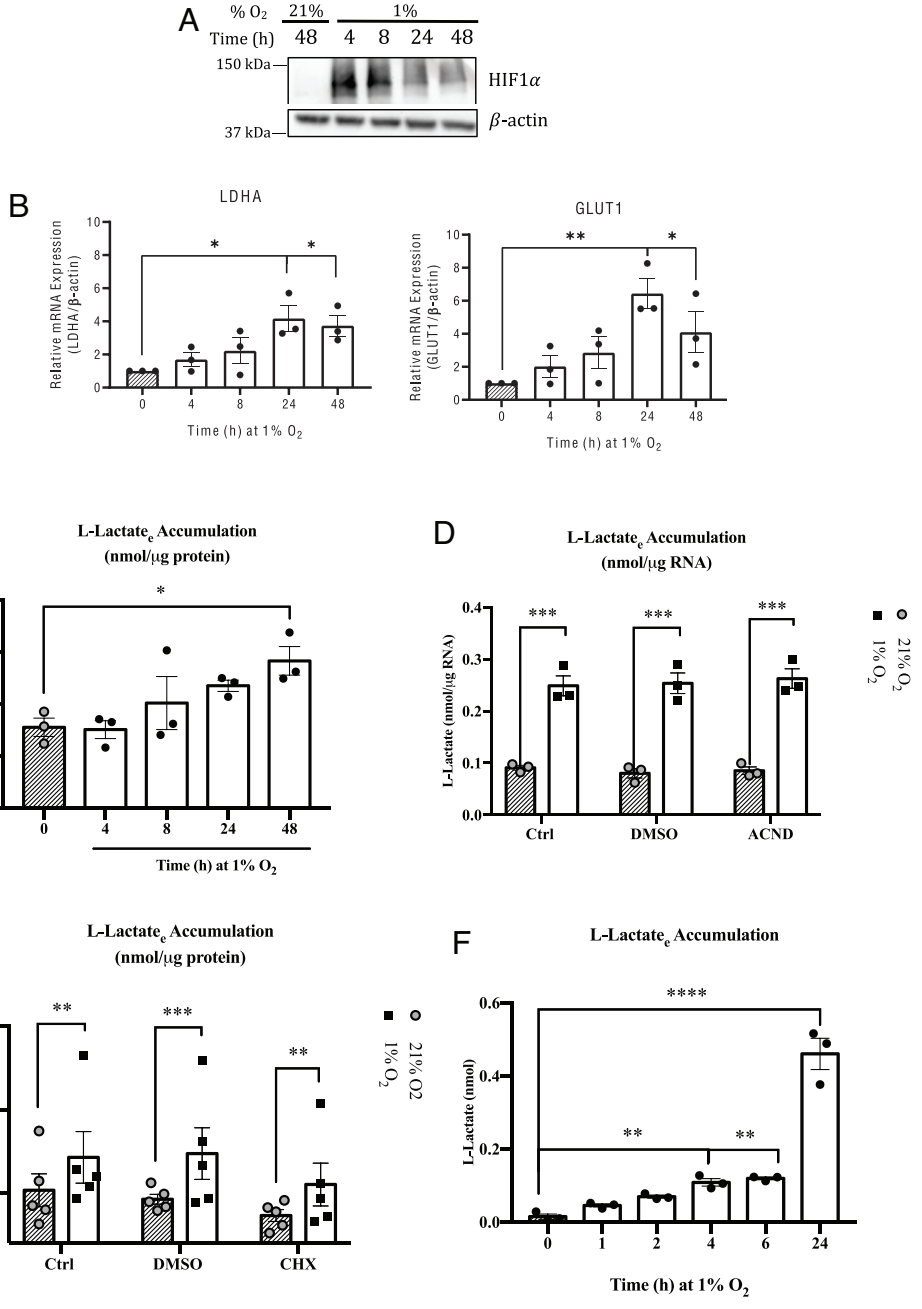


**Fig. 1.** Hypoxia-induced glycolysis occurs in cells where de novo transcription or translation is inhibited. (*A*) Representative immunoblots reflecting HIF-1α stabilization in Caco-2 cells exposed to 1% $O_2$ for 0 to 48 h. (*B*) LDHA and GLUT1 mRNA expression from Caco-2 cells exposed to 1% $O_2$ for 0 to 48 h (*C*) Lactate$_e$ accumulation from Caco-2 cells exposed to 21% $O_2$/1% $O_2$ 0 to 48 h (*D*) Lactate$_e$ accumulation in Caco-2 cells treated with 0 to 100 ng/mL of ACND or (*E*) 0 to 10 μg/mL of CHX prior to their exposure to 21% $O_2$ or 1% $O_2$ for 24 h. (*F*) Lactate$_e$ accumulation from human platelets exposed to 21% $O_2$/1% $O_2$ for 0 to 24 h. All data are shown as mean ± SEM. $n$ = 3 to 5 independent experiments. Statistical analyses were performed using a one- or two-way ANOVA, followed by the Holm–Sidak post hoc test.

(*SI Appendix*, Fig. S1). Furthermore, hypoxia strongly induced glycolysis in human platelets despite these cells being nonnucleated and therefore lacking the capacity for canonically transcriptional activity (Fig. 1*F*). Collectively, these data implicate a nontranscriptional element to hypoxia-induced glycolysis.

**GEs PFKP and HK2 Interact with GLUT1 in Hypoxia.** Having identified that hypoxia-induced glycolysis occurs in cells where de novo transcription and translation are inhibited, we next investigated potential nontranscriptional mechanisms of glycolytic induction in these cells. One possibility is that hypoxia alters the spatial organization of the glycolytic pathway to increase flux through the pathway. We examined the spatiotemporal organization of the glycolytic pathway using immunoprecipitation coupled to unbiased time-of-flight mass spectrometry (IP/MS). We analyzed the interactome of key rate-limiting GEs phosphofructokinase (PFK; platelet type isoform, PFKP) and pyruvate kinase (PK, M2 isoform; PKM2) isolated from protein homogenates of cells exposed to hypoxia or normoxia (Fig. 2 and *SI Appendix*, Fig. S3). Several proteins previously identified to interact with PFKP [e.g., ATP1A1 (22) or MTHFD1 (23)] or PKM2 [PSMD14/POH1 (24)] were readily detected in our screens, thereby supporting our experimental approach. Comparisons of the PFKP and PKM2 interactomes from both hypoxic- and normoxic-exposed cells revealed numerous hypoxia-sensitive interactions between PFKP and PKM2 and proteins involved in glucose metabolism including GLUT1, GLUT3, and HK2, particularly following 24 h and 48 h of hypoxic exposure (Fig. 2 *B* and *C* and *SI Appendix*, Fig. S3). Furthermore, chemically cross-linking proteins prior to immunoprecipitation using disuccinimidyl sulfoxide (DSSO; 5 mM) strongly increased the number of hypoxia-sensitive GEs identified in PFKP and PKM2 interactomes (*SI Appendix*, Figs. S2 and S3).

We confirmed the interactions identified in the PFKP IP/MS using both IP–western blot (Fig. 2*D*) and an in situ proximity ligation assay (PLA) (Fig. 3 and *SI Appendix*, Fig. S4). HK2 and PFKP both demonstrated a hypoxia-sensitive interaction with GLUT1 (Fig. 2*D* and *SI Appendix*, Fig. S4). Similarly, visualization of PFKP and HK2 colocalization using a PLA and confocal microscopy also revealed a greater level of PFKP/HK2 colocalization in hypoxic cells relative to normoxic controls (Fig. 3). These findings support the idea that hypoxia alters the spatial organization of glycolysis by promoting interactions between proteins involved in glucose metabolism. Interestingly, despite these interactions, hypoxic cells retained their metabolic flexibility through the pentose phosphate pathway (PPP) and remained capable of achieving redox balance (*SI Appendix*, Fig. S5).

**Knockdown of HIF-1α Abrogates Hypoxic Induction of Glycolysis.** We next sought to investigate the mechanisms by which hypoxia promotes the spatial reorganization of glucose-metabolizing proteins. In all metazoan species, adaptation to hypoxia is orchestrated by HIF, a transcription factor which becomes stabilized in hypoxia when functional proline hydroxylation by prolyl hydroxylase

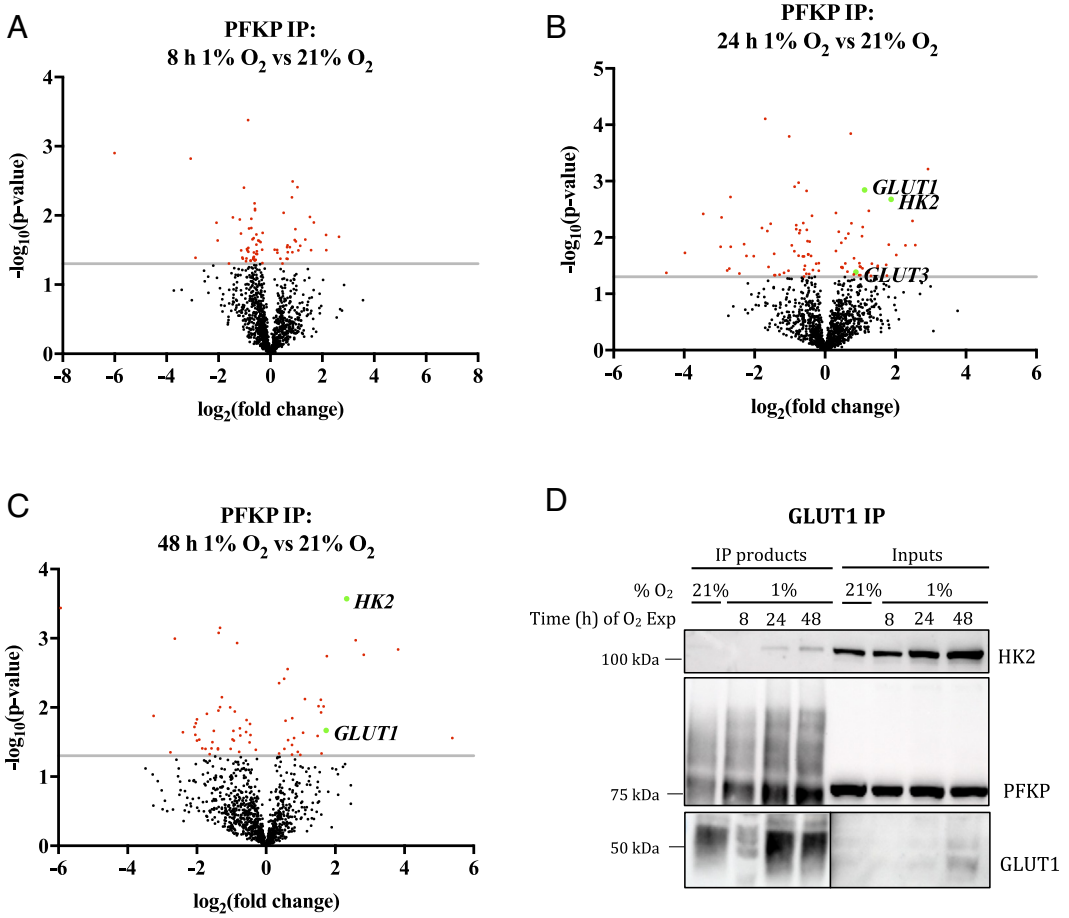


**Fig. 2.** Hypoxia increases interactions between proteins involved in glucose metabolism. (*A*–*C*) Volcano plots representing fold enrichment (LFQ intensity) of proteins identified in PFKP IP following exposure of cells to 1% $O_2$ for 8 h (*A*), 24 h (*B*), or 48 h (*C*) relative to normoxic PFKP IP. Proteins involved in glucose metabolism indicated in green. (*D*) Representative immunoblots reflecting HK2 and PFKP expression following co-IP of GLUT1 from whole cell lysates of Caco-2 cells exposed to 21%/1% $O_2$ for 8 to 48 h (Input = 5% total IP).

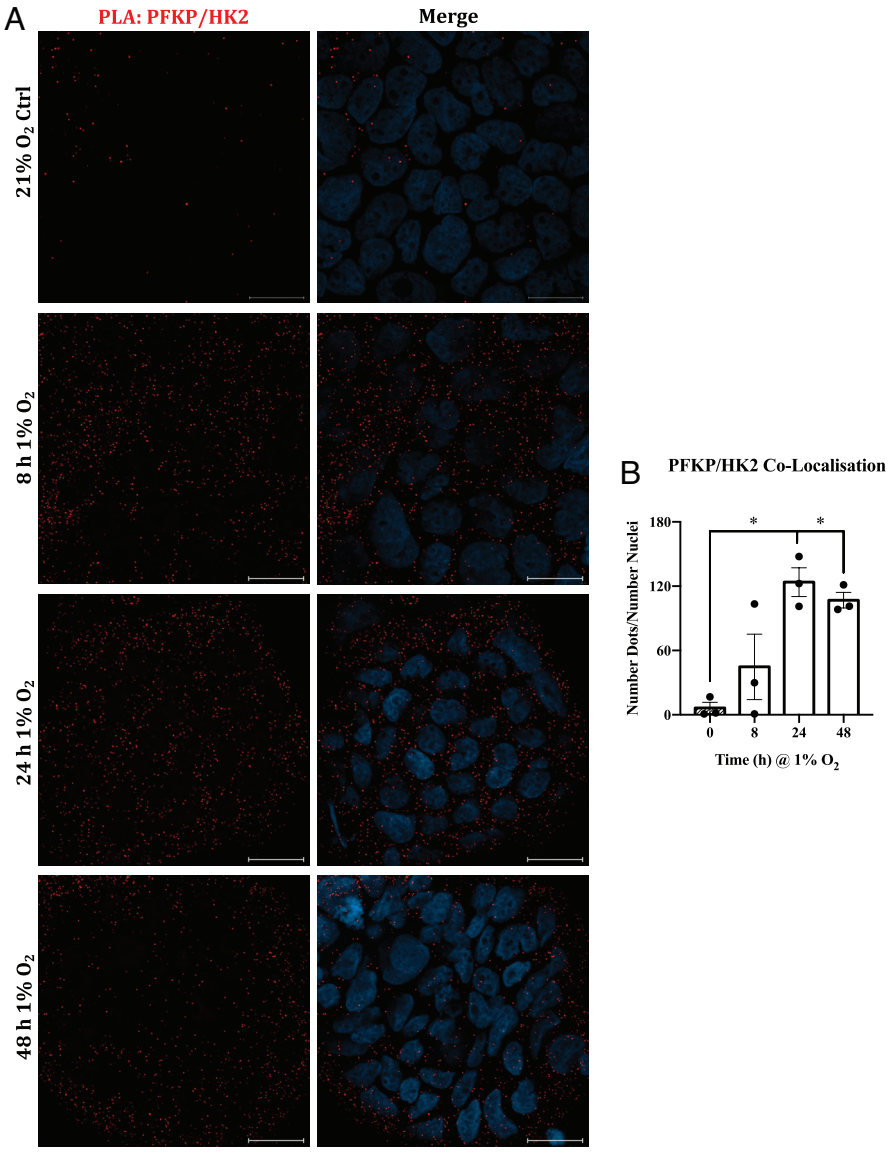


**Fig. 3.** Hypoxia promotes protein–protein interactions between GEs PFKP and HK2. (*A*) Representative PLA confocal images of Caco-2 cells exposed to 21%/1% $O_2$ for 0 to 48 h. PFKP and HK2 interactions indicated by a single red spot. Blue, Nuclear staining (DAPI). (Scale bar, 20 μm.) $n = 3$ independent experiments. (*B*) Quantification of PLA spots for each z-stack captured. Data are shown as mean ± SEM for $n = 3$ different fields of view for $n = 3$ independent experiments. Statistical analyses were performed using a one-way ANOVA, followed by the Holm–Sidak post hoc test.

domain (PHD) proteins becomes inhibited. We hypothesized that if the interactions observed were mediated by HIF-1α, then pharmacological inhibition of HIF-prolyl hydroxylases (leading to HIF stabilization) would be sufficient to promote glycolysis in normoxia. Inhibition of PHDs using the panhydroxylase inhibitor dimethyloxalylglycine (DMOG) promoted a time-dependent increase in HIF-1α stabilization (Fig. 4*A*) and increased basal glycolysis in the absence of hypoxia (Fig. 4*B*). Interestingly, while DMOG increased glycolysis, dual stimulation of cells with hypoxia and DMOG did not have an additive effect on glycolytic induction (Fig. 4*C*), suggesting that pharmacological inhibition of PHDs phenocopies the hypoxia-induced enhancement of glycolysis. As HIFs are the primary targets for functional proline hydroxylation in eukaryotic cells (25, 26), we investigated the role of HIF-1α in DMOG-induced glycolysis. HIF-1α was selectively knocked down using specific siRNA oligonucleotides against HIF-1A (siHIF-1A). Knock-down efficiency was confirmed at both the protein level (Fig. 4*D*) and using an (hypoxia-responsive element) HRE-*Gaussia* Luciferase reporter system (Fig. 4*E*). Knockdown of HIF-1α completely abolished DMOG-induced glycolysis (Fig. 4*F*). These results implicate HIF-1α as a primary mechanism by which DMOG and hypoxia induce glycolysis. These data, together with the identification that hypoxia-induced glycolysis can proceed in the absence of de novo transcription or translation, led us to hypothesize a possible nontranscriptional role for HIF-1α in the promotion of glycolysis in hypoxia.

**Hypoxia-Induced Glycolysis Occurs in the Absence of HIF-1-Driven Transcriptional Activity.** HIF-1α induces glycolysis in hypoxia by transcriptionally up-regulating GEs and glucose transporters to promote an increased flux through the glycolytic pathway. This canonical induction of glycolysis by HIF-1α however does not explain the observation that glycolysis can be induced by hypoxia in the absence of de novo gene transcription or protein translation. We therefore hypothesized an additional nontranscriptional role for HIF-1α in mediating glycolysis in hypoxia. To dissect the transcriptional and nontranscriptional activities of HIF-1α, we utilized a clone of Caco-2 cells stably transfected with a single guide RNA (sgRNA) targeting the basic helix–loop–helix domain of endogenous HIF-1A, which are designated HIF-1A NT (nontranscriptional) cells. While the abundance of HIF-1α was not affected by this genetic modification (Fig. 5*A*), this clone showed no induction of HIF-1-dependent gene expression at the protein level in response to hypoxia (Fig. 5*A*) and no induction of HIF-1 reporter activity in response to DMOG treatment (Fig. 5*B*). However, these cells remained capable of inducing glycolysis following their

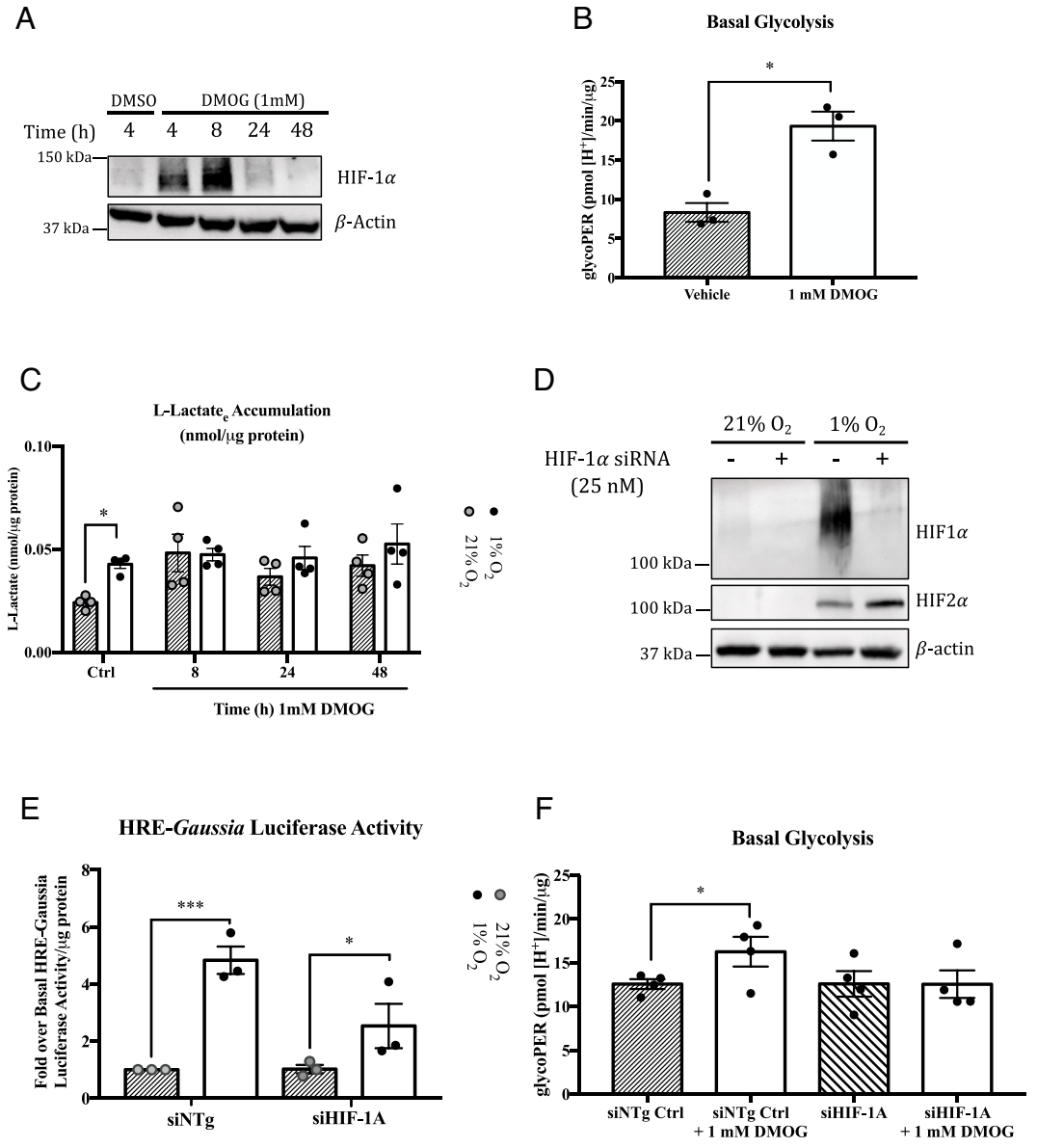


**Fig. 4.** Hydroxylase inhibition induces glycolysis in Caco-2 cells via HIF-1α (*A*) Representative immunoblots of HIF-1α stabilization in Caco-2 cells treated with 1 mM DMOG for 4 to 48 h. (*B*) Basal glycolytic levels quantified for Caco-2 treated with 1 mM DMOG for 24 h. (*C*) L-Lactate$_e$ accumulation in Caco-2 cells pretreated with 1 mM DMOG for 8 to 48 h and exposed to 1%/21% $O_2$ for 24 h. (*D*) HIF-1α and HIF-2α stabilization determined using western blot in Caco-2 cells transfected with 25 nM siHIF-1A/siNTg Ctrl and exposed to 1% $O_2$ for 24 h. (*E*) HIF-1α functional activity in Caco-2 cells cotransfected with an HRE-*Gaussia* Luciferase reporter construct and siHIF-1A/siNTg Ctrl and exposed to 1% $O_2$ for 24 h. Results shown as normalized RLU over normalized basal (NTg Ctrl siRNA–treated normoxic cells) RLU. (*F*) Basal glycolysis of siRNA transfected Caco-2 cells treated with 1 mM DMOG for 24 h quantified prior to first injection. All data are shown as mean ± SEM for a minimum of $n$ = 3 independent experiments. Statistical analyses were performed using a one- or two-way ANOVA, followed by the Holm Sidak post hoc test.

exposure to hypoxia, as indicated by increased lactate$_e$ accumulation (Fig. 5*C*). This finding not only supports our prior observations that hypoxia-induced glycolysis can proceed in the absence of global de novo gene transcription or protein translation (Fig. 1) but further suggests that specifically inhibiting the HIF-1-driven upregulation of GEs and proteins which support glucose metabolism is sufficient to replicate this phenotype. Interestingly, this response could be reversed in the presence of siHIF-1A (Fig. 5*D*) suggesting that although hypoxia-induced glycolysis can proceed in the absence of HIF-1-driven transcription, the HIF-1α protein is necessary for hypoxia-induced glycolysis to proceed. Collectively, these data suggest that HIF-1α may play an additional nontranscriptional role in promoting hypoxia-induced glycolysis.

**Cytosolic HIF-1α Interacts with Proteins That Support Glucose Metabolism in a Hypoxia-Sensitive Manner.** To investigate a potential nontranscriptional mechanism by which HIF-1α may regulate hypoxia-induced glycolysis, we analyzed the interactome of cytosolic HIF-1α. Using subcellular fractionation to separate nuclear and cytosolic fractions, we isolated the cytosolic fractions from hypoxic- or normoxic-exposed Caco-2 cells, immunoprecipitated cytosolic HIF-1α, and analyzed its interactome using unbiased mass spectrometry (Fig. 6). We identified several hypoxia-sensitive, known interactants of HIF-1α (e.g., von-Hippel Lindau tumor suppressor protein (VHL) and Aryl hydrocarbon Receptor Nuclear Translocator (ARNT)) in our analyses, supporting the sensitivity of our IP/MS approach (Fig. 6 *A*–*C*). Interestingly, HIF-1α also interacted with several GEs and glucose transporters within the cytosol in a hypoxic-sensitive and time-dependent manner. These interactants were confirmed independently using coimmunoprecipitation–western blot analysis (Fig. 6 *D* and *E*), where GLUT1, PFKP, and HIF-1α displayed hypoxia-sensitive interaction. Finally, these interactions were also observed in our HIF-1α IP from our HIF-1A NT clone (Fig. 6*F*, input protein lysates from cytosolic fractions Fig. 6*G*), suggesting that these interactions between HIF-1α, GEs, and glucose transporters can occur independent of HIF-1-driven transcription.

## Discussion

Hypoxia-induced glycolysis canonically occurs via an HIF-1-dependent transcriptional upregulation of GEs and glucose transporters (27) and complementary HIF-1-mediated suppression of

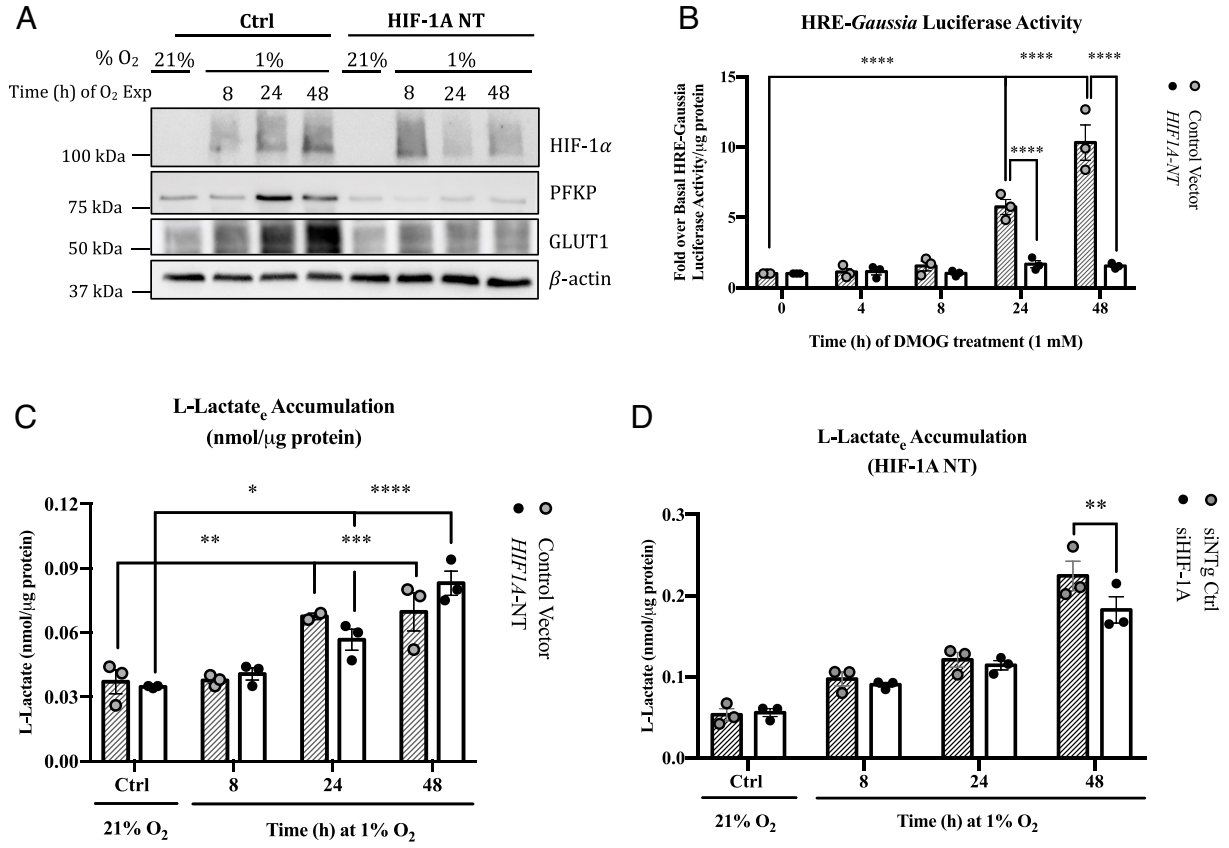


**Fig. 5.** Hypoxia-induced glycolysis occurs in cells where *HIF-1A* is transcriptionally inactive. (*A*) Representative immunoblots reflecting HIF-1α stabilization in whole cell lysates generated from hypoxic/normoxic empty vector control/HIF-1A NT cells. (*B*) Quantification of HIF-1α functional activity in control/HIF-1A NT cells transfected with an HRE-*Gaussia* Luciferase reporter construct and treated with DMOG (1 mM) for up to 48 h. (*C*) Lactate$_e$ accumulation from control/HIF-1A NT cells exposed to 21% $O_2$/1% $O_2$ for 0 to 24 h. (*D*) Lactate$_e$ accumulation from HIF-1A NT cells exposed to 21% $O_2$/1% $O_2$ for 0 to 48 h in the presence of siHIF-1α or siNTg Ctrl. All data are shown as mean ± SEM. *n* = 3 independent experiments. Statistical analyses were performed using a two-way ANOVA followed by the Holm–Sidak post hoc test.

oxidative phosphorylation (28, 29). This transcriptional upregulation of glycolysis serves to maintain ATP production in the absence of tricarboxylic acid cycle activity. Once up-regulated, the enzymes involved in glycolysis have been extensively described to diffuse freely throughout the cytoplasm of mammalian cells. However, in the context of hypoxia, an energetically demanding environment, relying solely on a transcriptional upregulation may not be sufficient to sustain glycolysis as the primary method of ATP generation. An increased expression alone would necessitate each enzyme of the glycolytic pathway relying on a rapid equilibration of substrate levels across a relatively vast aqueous cellular cytosol to allow for increased pathway activity. It therefore seems unlikely that without any additional organization or localization of pathway components, the metabolism of glucose would be an effective metabolic strategy, particularly in an energy-demanding and $O_2$-deprived cellular environment.

In this study, we demonstrate that both primary platelets and intestinal epithelial cells can induce glycolysis in hypoxia even in the absence of functional transcriptional machinery, suggesting that additional nontranscriptional mechanisms are involved in mediating this metabolic shift to glycolysis in hypoxia. When considering a nontranscriptional mechanism for glycolytic induction, we hypothesized that hypoxia may alter the spatial organization of GEs to promote protein–protein interactions between pathway enzymes which may maximize the catalytic efficiency of the pathway by promoting direct substrate channeling of glycolytic intermediates between sequential pathway enzymes (Fig. 7). The reorganization of GEs into a heteromultimeric protein complex has long been postulated as a means to regulate glucose metabolism, particularly during periods of cellular stress, with a large body of cross-kingdom evidence existing for the formation of such complexes (30). Here, we provide evidence that hypoxia alters the spatial organization of glycolysis to promote hypoxia-sensitive interactions between GEs and glucose transporter in the formation of an enzymatic complex. While these interactions may allow for more efficient regulation of flux through the glycolytic pathway in hypoxia, future studies will address the functional implication of these interactions. Interestingly, although the GE interactions identified here were induced by hypoxia, there is evidence to suggest that a basal level of interaction exists between GEs and glucose transporters in normoxia. This implies that these interactions may not occur as a binary event but in a dynamic manner depending on the energetic requirements of a cell, tissue, or overall organism.

Although the formation of a glycolytic complex may provide cells with a means to coordinate glucose metabolism in hypoxia, it is important to consider the effect of these interactions on the metabolic flexibility of shunt pathways, such as pathways responsible for NADPH generation (e.g., PPP). In our studies, glucose-6-phosphate dehydrogenase (G6PD) (the committed enzyme of the PPP) is not down-regulated by hypoxia and cells remain capable of achieving redox balance. This suggests that like other organisms where glycolytic complexes are observed, PPP activity is not adversely affected by these interactions. We hypothesize that hypoxic cells may distribute their glucose for metabolism via an interplay between glycolysis and the PPP depending on the cells' relative need for ATP and/or reductive power. Future work

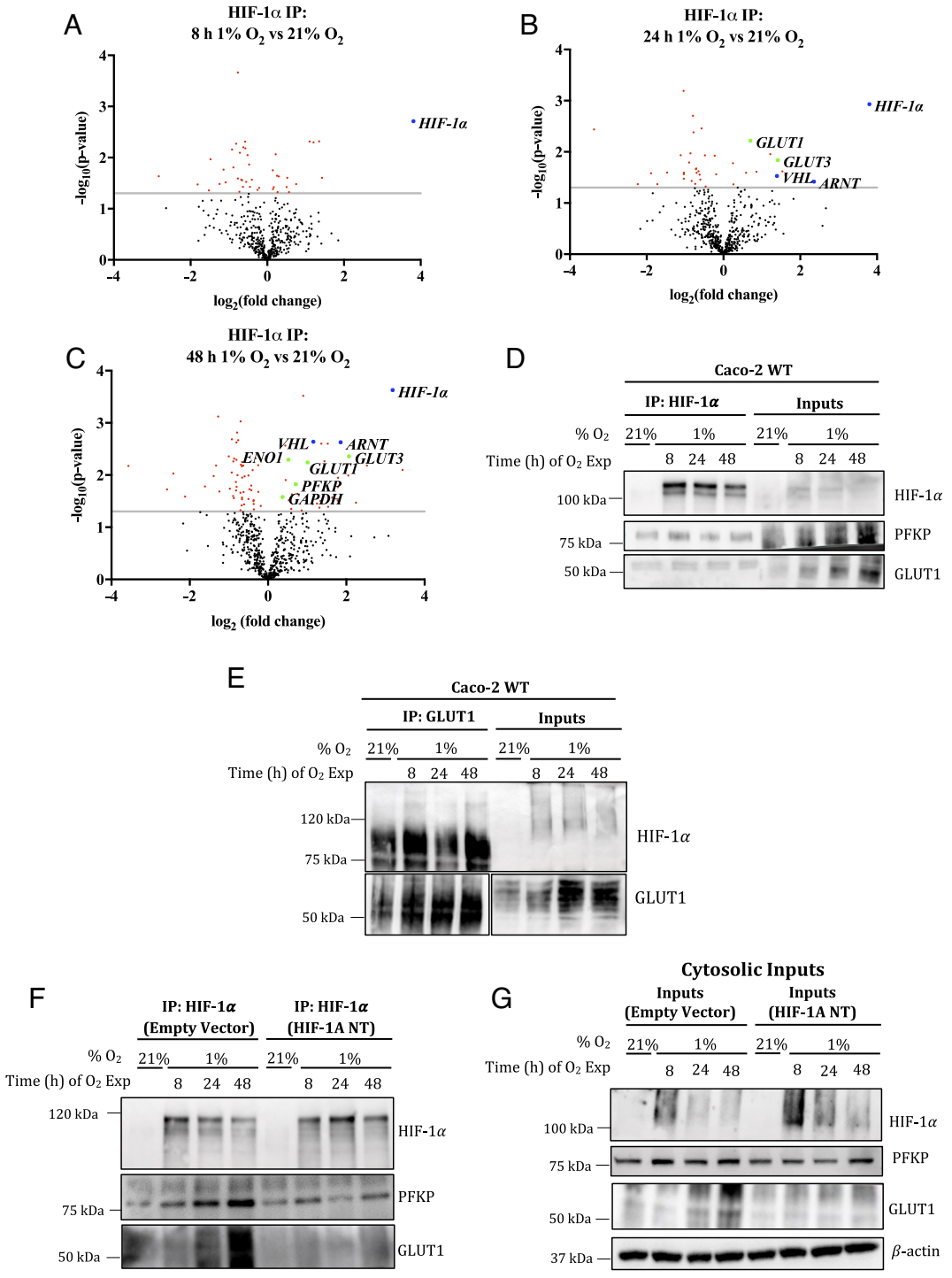


**Fig. 6.** Hypoxia increases interactions between cytosolic HIF-1α and proteins involved in glucose metabolism. (*A–C*) Volcano plots representing fold enrichment (LFQ intensity) of proteins identified in cytosolic HIF-1α IP following exposure of cells to 1% $O_2$ for 8 h (*A*), 24 h (*B*), or 48 h (*C*) relative to normoxic HIF-1α IP (21% $O_2$). Blue, Proteins understood to interact with HIF-1α. Purple, Proteins involved in glucose metabolism (*D* and *E*) Representative immunoblots reflecting GLUT1, PFKP, and HIF-1α expression following co-IP of HIF-1α (*D*) or GLUT1 (*E*) from cytosolic hypoxic/normoxic wild-type Caco-2 cell fractions or (*F*) cytosolic HIF-1A NT Caco-2 cell fractions. (*G*) Cytosolic inputs for (*F*). Inputs = 10% IP for (*D–G*).

will focus on addressing whether the interactions identified positively regulate glycolysis in hypoxia and, if so, the precise mechanism(s) by which redox balance is achieved.

Our metabolic analyses, consistent with other studies (31), suggest that the hypoxic induction of glycolysis, as a whole, is an HIF-1α-dependent mechanism. However, we present multiple lines of experimental evidence which suggest that this induction of glycolysis can occur independent of HIF-1-driven transcriptional activity. While HIFs are conventionally known for their role in mediating hypoxia-induced transcriptional changes, evidence of nontranscriptional roles for both HIF-1α and HIF-2α has been previously reported (32–34). The involvement of HIF-1α in a nontranscriptional induction of glycolysis may explain why loss of HIF-1β does not perturb the hypoxic glycolytic phenotype in certain cell types (35, 36), whereas loss of HIF-1α does (31). However, given that HIF-1α expression is dispensable for the hypoxia-induced

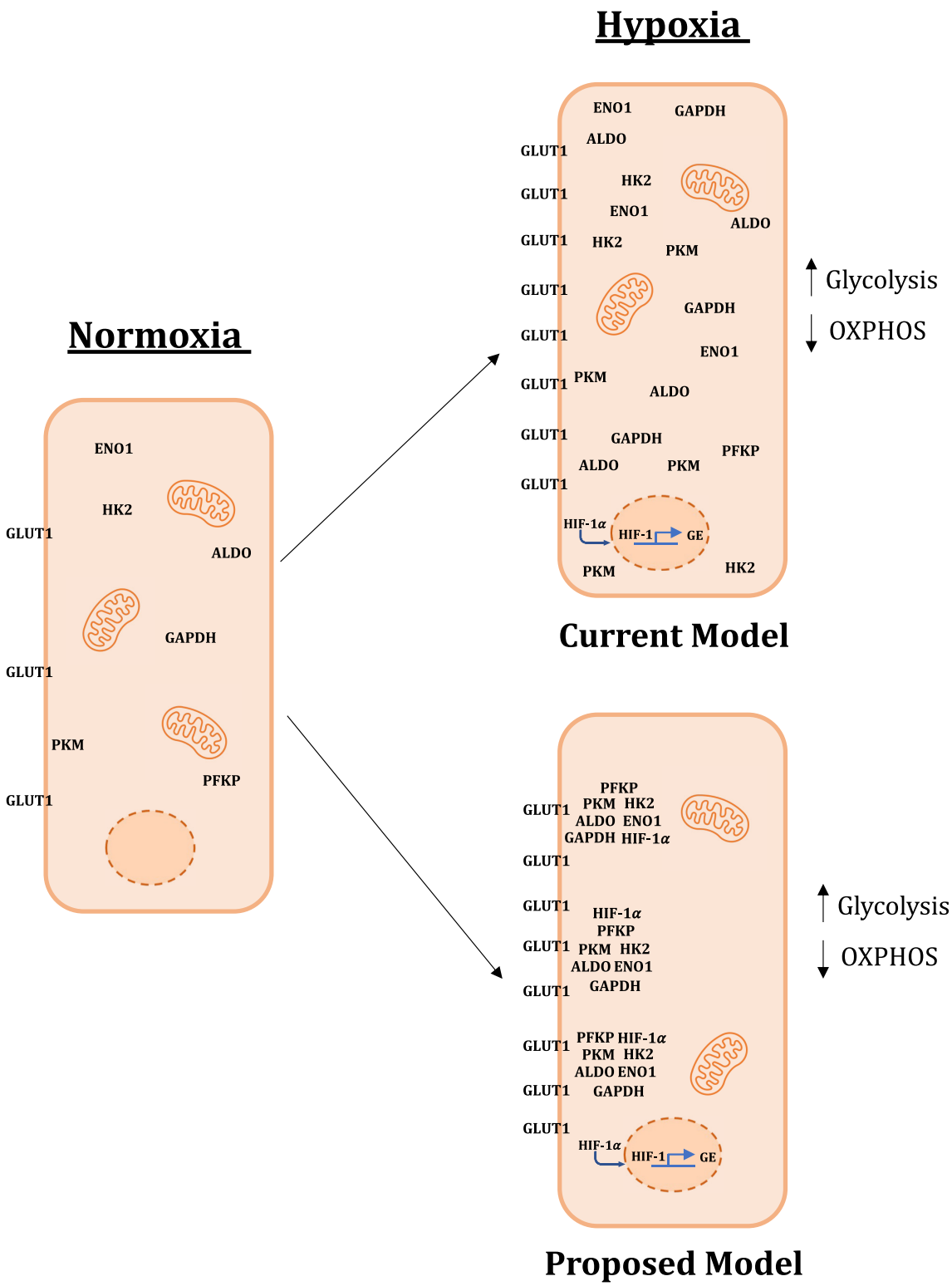


**Fig. 7.** Proposed mechanism for hypoxia-induced glycolysis. The canonical model for hypoxia-induced glycolysis involving HIF-1-driven transcriptional upregulation of glucose transporters and GEs (GE) within the cell (*Top Right*). Our proposed model (*Bottom Right*) suggestive of an additional layer of complexity in this response, in a nontranscriptional, spatial reorganization of GEs, glucose transporters, and HIF-1α into a metabolic complex which may facilitate glucose metabolism and adaption to hypoxic stress.

glycolytic phenotype in other cell types (37), we now require a more comprehensive understanding of the complete mechanisms by which HIF-1α can induce glycolysis in hypoxia. Importantly, although we provide evidence that cytosolic HIF-1α interacts with this glycolytic complex, the biological significance of these interactions remains unclear. HIF-1α may play a role in driving complex formation, or recruitment of HIF-1α may play a role in stabilizing glycolytic complexes already formed by another mechanism. Future research will focus on elucidating the precise role of HIF-1α in glycolytic complex formation and/or maintenance.

The identification of this nontranscriptional mechanism which complements the transcriptional regulation of glycolysis supports the

idea that metabolism may rely on the integration of numerous complementary mechanisms at various stages of a given metabolic pathway for maximum bioenergetic efficacy. However, several questions remain in developing our understanding of this nontranscriptional induction of glycolysis in hypoxia. First, it is crucial to determine whether these interactions positively regulate glycolysis in hypoxic cells by facilitating substrate channeling through the glycolytic pathway. Existing evidence strongly suggests that glycolytic activity is most efficient when sequential enzymes are in close proximity (38). In the context of hypoxia, channeling of glucose through glycolysis to increase ATP production from glycolysis would be highly beneficial for maintaining bioenergetic homeostasis. Second, further research is required to determine the specific subcellular localization of this complex. The formation of this complex in subcellular regions of high energy demands may be beneficial in promoting localized ATP production in support of various biological processes, particularly during periods of metabolic stress. Finally, understanding how these interactions occur is an area of key interest. There is evidence indicating that glycolytic complexes in other organisms can form as phase-separated biomolecular condensates (39), as peroxisome-like, membrane-bound vesicles (40), and elsewhere, using RNAs as a structural scaffold for complex formation (15, 21). Understanding the structural composition of this complex may provide us with further insight into its regulation.

In summary, in this study, we highlight a hypoxia-dependent, nontranscriptional component to the regulation of glycolysis. We propose that this nontranscriptional regulation is achieved via a spatial reorganization of proteins involved in glucose metabolism into a heteromultimeric protein complex which may promote glucose metabolism and cellular metabolic adaptation to hypoxic stress.

## Materials and Methods

**Cell Culture.** Caco-2 cells (ATCC®, HTB-37™) were used as in vitro representatives of intestinal epithelial cells. Caco-2 cells were cultured in DMEM containing 4.5 g/L glucose, 10% FBS, 1% MEM nonessential amino acids, and 1% penicillin–streptomycin (100 U/mL). Cells were maintained in a humidified atmosphere of ambient air supplemented with 5% $CO_2$ and maintained at 37 °C.

Cells were exposed to hypoxia by placing cells into normobaric glove-box chambers (Coy Laboratories, USA) preequilibrated to 1% $O_2$, 5% $CO_2$, and 37 °C. Primary platelets were placed on an orbital shaker within the chamber to mimic sheer stress.

**CRISPR-Cas9 Editing of Caco-2 Cells.** sgRNAs for HIF-1A (sequence 5′-GATGGTAAGCCTCATCACAG-3′) were designed via Benchling© online platform and cloned in pLenti-sgRNA backbone (Addgene, 71409), as described by ref. 41. For generating a stable Caco-2-iCas9 cell line, cells were incubated with 1 mL lentivirus suspension, supplemented with 8 μg/mL polybrene (Sigma-Aldrich, TR-1003) before selection with Neomycin (2 mg/mL) for 7 d. For introduction of sgRNA, Caco-2-iCas9 cells were incubated with 1 mL lentivirus containing sgRNA (empty vector or against HIF-1A), supplemented with 8 μg/mL polybrene. Then, 24 h after infection, selection of transfected cells was performed with 20 μg/mL puromycin for 7 d. The resulting mutant Caco-2 cell line was cultured at low density in Glutamax™ DMEM, clones were picked and expanded, and DNA, RNA, and protein were collected for sequencing and functional validation of stable transfection.

**Isolation of Primary Platelets.** Studies using primary human platelets were approved by the University College Dublin Human Research Ethics Committee (LS-19-68-Smolenski). Venous blood was collected from the antecubital veins of healthy donors who had given their informed consent on the day of donation. Blood was drawn into prewarmed (37 °C) CCD-EGTA buffer (100 mM trisodium citrate, 7 mM citric acid, 140 mM D-glucose, and 15 mM EGTA). To isolate platelets, samples were centrifuged at 200 × g for 15 min (braking mechanism inactivated). The platelet-rich plasma was removed and centrifuged at 600 × g for a further 15 min (braking mechanism activated). Pelleted platelets were resuspended in prewarmed resuspension buffer (145 mM NaCl, 5 mM KCl, 1 mM $MgCl_2$, 10 mM HEPES, and 10 mM D-glucose, pH 7.4) and plated evenly onto 60-mm dishes for hypoxic exposures.

**Reagents.** Actinomycin-D (ACND) and cycloheximide (CHX) (Sigma A9415 and C4859) were used to inhibit gene transcription or protein translation, respectively. For inhibition of HIF prolyl-hydroxylases, DMOG (Cayman Chemical, 71210) was used. To inhibit the mitochondrial electron transport chain, rotenone (Sigma, R8875) was used.

**Subcellular Fractionation.** For subcellular fractionation studies, cells were lysed in cytosolic lysis buffer (10 mM HEPES pH 8, 1 mM $MgCl_2$, 10 mM KCl, 200 mM sucrose, 1% NP40, supplemented with protease inhibitors) and centrifuged at 12,000 rpm for 5 min at 4 °C. The resulting supernatant contained the cytosolic fraction. Pelleted cells were resuspended in nuclear lysis buffer (20 mM HEPES pH 8, 1.5 mM MgCl2, 420 mM NaCl, 0.2 mM EDTA, 0.5 mM DTT, 10% glycerol, supplemented with protease inhibitors), incubated on ice for 30 min with gentle agitation and subsequently centrifuged at 14,000 rpm for 5 min at 4 °C. The resulting supernatant contained the nuclear fraction.

**RNA Interference.** Caco-2 cells were cultured to 30% confluence and transfected with 25 nM of oligonucleotides against HIF-1α (ON-TARGETplus SMARTpool, Dharmacon (L-004018-00-0020) or control ON-TARGETplus Nontargeting Pool (Dharmacon, D-001810-10-05) in antibiotic-free media for 48 h prior to their exposure to hypoxia.

**L-Lactate Assay.** Extracellular L-Lactate ($lactate_e$) accumulation was quantified using an L-Lactate Assay (Abcam, abcam65331), carried out according to the manufacturer's instructions. Absorbance was measured at OD 450 nm. Where indicated, L-$Lactate_e$ levels (nmol) are presented normalized to protein content (μg) for comparison of apparent metabolic rates.

**HRE-Gaussia Luciferase Reporter Assay.** HIF-1α functional activity levels were determined using a HRE-*Gaussia* Luciferase reporter system. Caco-2 cells were transfected with 750 ng of the HRE-*Gaussia* Luciferase reporter construct for 24 h in antibiotic-free media prior to their exposure to hypoxia. Secreted bioluminescence, indicative of HRE activity, was quantified using the Pierce™ *Gaussia* Luciferase Glow Assay Kit (Thermo Scientific, 16161). Relative Luminescence Units (RLU) are presented normalized to total protein content (μg) for comparison of apparent HIF-1α functional activity.

**Real-Time Metabolic Measurements.** Glycolytic rate was quantified in cells using the Glycolytic Rate extracellular flux assay (Agilent, 103346-100) and the Seahorse XF HS Mini Analyzer (Agilent, California, USA) according to the manufacturer's instructions. Data were analyzed using Seahorse Analytics (Agilent) and are presented normalized to protein content (μg) for comparison of apparent metabolic rates.

**Reverse Transcriptase Quantitative PCR.** RNA was isolated from hypoxic/normoxic Caco-2 cells using TRI Reagent (Sigma, T9424). cDNA was synthesized from 1 mg total RNA using M-MLV Reverse transcriptase. Target cDNAs were amplified and quantified using SYBR Green chemistry on the Applied Biosystems Quantstudio 7 Flex PCR system. Thermal cycles were one 10-min cycle at 95 °C, followed by heating samples to 95 °C for 15 s and cooling to 60 °C for 1 min for a further 40 cycles. Relative gene expression was calculated using the δ-δ Ct method. SYBR Green primer sequences can be found in *SI Appendix*, Table S1.

**Immunoblotting.** Whole-cell protein lysates were generated by lysing cells in whole-cell lysis buffer (100 mM Tris-HCl, 300 mM NaCl, 10 mM $MgCl_2$, 1% Triton X-100 supplemented with protease inhibitors). Isolated proteins were denatured, reduced, and separated by sodium dodecyl sulfate–polyacrylamide gel electrophoresis after which they were immunoblotted for proteins of interest using standard protocols. Primary antibodies against GLUT1 (CST #12939, 1:1,000 or Invitrogen MA5-11315, 1:500), HK2 (Invitrogen MA5-15679, 1:1,000), PFKP (CST #8164, 1:1,000) HIF-1α (CST #36169, 1:500 or BD Biosciences #610958, 1:500), Nrf2 (CST #12721, 1:1,000), G6PD (Proteintech 25413-1-AP, 1: 1,000), MTHFD2 (CST #98116, 1:1,000), β-actin (Sigma A5441, 1:5,000) were used alongside species-specific HRP-conjugated secondary antibodies [CST #7074 (Anti-Rabbit IgG), #7076 (Anti-Mouse IgG)]. The resulting signal was detected using enhanced chemiluminescence (Advansta WesternBright HRP Substrate) and imaged using the Vilber Fusion FX Chemiluminescent Imager.

**In Situ PLA.** Caco-2 cells (Wild-type, HIF-1A NT, or Empty Vector control) were seeded onto poly-D-lysine (Thermo-Fisher, A3890401)-coated 10-mm coverslips placed into sterile 48-well plates and exposed to hypoxia/normoxia as described above. Cells were fixed using 4% paraformaldehyde (pH 7.4). Fixed cells were removed from the chamber, permeabilized for 15 min in DPBS-0.3% Triton X-100 at room temperature and blocked in Duolink® Blocking Buffer (Merck) for 60 min in a heated humidified atmosphere (37 °C). Samples were incubated with primary antibodies against PFKP (Invitrogen, PA5-84295, 1:300), HK2 (Invitrogen, MA5-15679, 1:200), or GLUT1 (Invitrogen, MA5-11315, 1:600) diluted in Duolink® Antibody Diluent overnight at 4 °C. Samples were then incubated with oligonucleotide-conjugated secondary antibodies in a heated (37 °C) humidified atmosphere for 60 min. For hybridization of probes, a ligation solution consisting of two bridging DNA oligonucleotides and a ligase were added to all samples for 30 min (37 °C), followed by an amplification solution to produce a signal easily detectable using fluorescence microscopy. For visualization of nuclei, cells were counterstained using nucleic acid stain DAPI (750 ng/mL) for 10 min at room temperature. Once stained, coverslips were inverted and mounted onto glass slides. Z-stacks were acquired using a Zeiss LSM800 laser-scanning confocal microscope using a 63X oil immersion objective. PLA spots were quantified in a 3D-rendered z-stack acquired from 4 fields of view per biological replicate ($n = 3$) using the "Spots" function of Imaris software. DAPI-stained nuclei were counted to determine the number of cells per image. The number of spots present in each z-stack relative to cell number was determined for all technical and biological replicates to yield a mean PLA signal per condition.

**Immunoprecipitation-Coupled Western Blot.** Isolated proteins were quantified using the Bio-Rad DC™ Protein Assay (Bio-Rad, California, USA) and normalized to 1 mg of protein. Normalized lysates were incubated with a primary antibody against the protein of interest for 16 h at 4 °C with end-to-end rotation. To isolate antibody-bound proteins, 20 μL of Protein A agarose beads (Cell Signaling Technology, #9863) were added to each sample and incubated for 4 h at 4 °C. To remove nonspecific interactors, agarose beads were washed thrice using detergent-free IP wash buffer (100 mM Tris-HCl, 300 mM NaCl, and 10 mM $MgCl_2$). For western blot analysis, antibody-bound proteins were eluted by heating samples to 95 °C in NuPAGE™ LDS sample buffer (Thermo Fisher NP0007) for 10 min with 300 rpm. Beads were pelleted, supernatant was removed, and samples were further reduced by adding 100 mM DTT to each sample and heating for a further 5 min at 95 °C.

**Immunoprecipitation-Coupled Mass Spectrometry.** After coimmunoprecipitation, enzymatic digestion and elution of bead-bound proteins was performed as described by ref. 42. For reliable analysis of the specificity of interacting proteins, a bead-only control was characterized for every experiment to identify proteins which bind to the beads nonspecifically. Samples were desalted using C18 stagetips (43) and resuspended in 2.5% acetonitrile and 0.5% acetic acid buffer. Once desalted, 500 ng peptides were loaded onto Evotips as per the manufacturer's instructions (EvoSep). Samples were analyzed by the Mass Spectrometry Resource in University College Dublin on a Bruker TimsTOF Pro mass spectrometer connected to an EvoSep One chromatography system.

**Mass Spectrometry Protein Identification.** Raw data were processed using MaxQuant (44, 45), incorporating Andromeda search engine (46). Briefly, mass spectra were searched against a human database (Uniprot HUMAN) using a false discovery rate of 1% at the peptide and protein level. For the generation of label-free quantitative (LFQ) ion intensities for protein profiles, signals of corresponding peptides in different nano-HPLC MS/MS runs were matched by MaxQuant in a maximum time window of 1 min (47). Mass spectrometry data have been deposited to the ProteomeXchange Consortium via the PRIDE (8) partner repository with dataset identifiers PXD036950 (Dataset 1), PXD037020 (Dataset 2) and PXD037115 (Dataset 3).

**Statistical Analyses.** Mass spectrometry data were analyzed using Perseus (48). Briefly, LFQ values were $\log_2$ transformed, filtered for reverse and contaminants, and missing values were imputed from a normal distribution (width = 0.3; shift = 1.8). A two-sample test was applied using a *P*-value of $\alpha = 0.05$ for truncation.

Elsewhere, data are shown as mean ± SEM. Statistical significance was determined using either a one- or two-way ANOVA, followed by the Holm–Sidak post hoc test or paired *t* test where appropriate. Asterisks denote the level of significance such that $*P \le 0.05$, $**P \le 0.01$, $***P \le 0.001$, $****P \le 0.0001$.

**Data, Materials, and Software Availability.** Mass spectrometry proteomics data sets have been deposited in ProteomeXchange (PXD036950, PXD037020, PXD037115) (49–51).

**ACKNOWLEDGMENTS.** S.J.K. is funded by a University College Dublin Advance PhD Course Scheme grant awarded to C.T.T. (R19448). We thank Mathilde J. C. Broekhuis and Prof. Floris Foijer from the iPSC and CRISPR-Cas9 Facilities at the Laboratory of Ageing Biology and Stem Cells, European Research Institute for the Biology of Ageing, University Medical Center Groningen, University of Groningen (Groningen, the Netherlands) for assisting with generation of HIF-1A NT cell line. We thank Dr. Dimitri Scholz and the University College Dublin Conway Institute Imaging Core Facility for imaging support and services.

1. S. J. Kierans, C. T. Taylor, Regulation of glycolysis by the hypoxia-inducible factor (HIF): Implications for cellular physiology. *J. Physiol.* **599**, 23–37 (2020), 10.1113/JP280572.
2. L. A. O'Neill, D. G. Hardie, Metabolism of inflammation limited by AMPK and pseudo-starvation. *Nature* **493**, 346–355 (2013).
3. G. Eelen *et al.*, Endothelial cell metabolism. *Physiol. Rev.* **98**, 3–58 (2018).
4. N. N. Pavlova, C. B. Thompson, The emerging hallmarks of cancer metabolism. *Cell Metab.* **23**, 27–47 (2016).
5. A. R. Henderson, Biochemistry of hypoxia: Current concepts. I. An introduction to biochemical pathways and their control. *Br. J. Anaesth.* **41**, 245–250 (1969).
6. A. R. Fernie, Y. Zhang, L. J. Sweetlove, Passing the baton: Substrate channelling in respiratory metabolism. *Research (Wash. D.C.)* , 1539325 (2018).
7. Y. Zhang, A. R. Fernie, Resolving the metabolon: Is the proof in the metabolite? *EMBO Rep.* **21**, e50774 (2020).
8. S. Arrivault *et al.*, Dissecting the subcellular compartmentation of proteins and metabolites in arabidopsis leaves using non-aqueous fractionation. *Mol. Cell Proteomics* **13**, 2246–2259 (2014).
9. L. J. Sweetlove, A. R. Fernie, The spatial organization of metabolism within the plant cell. *Annu. Rev. Plant Biol.* **64**, 723–746 (2013).
10. N. Miura *et al.*, Spatial reorganization of Saccharomyces cerevisiae enolase to alter carbon metabolism under hypoxia. *Eukaryot. Cell* **12**, 1106–1119 (2013).
11. M. Jin *et al.*, Glycolytic enzymes coalesce in G bodies under hypoxic stress. *Cell Rep.* **20**, 895–908 (2017).
12. W. Quinones *et al.*, Structure, properties, and function of glycosomes in Trypanosoma cruzi. *Front. Cell Infect. Microbiol.* **10**, 25 (2020).
13. P. A. M. Michels, M. Gualdron-Lopez, Biogenesis and metabolic homeostasis of trypanosomatid glycosomes: New insights and new questions. *J. Eukaryot. Microbiol.* **69**, e12897 (2022), 10.1111/jeu.12897.
14. S. Jang *et al.*, Glycolytic enzymes localize to synapses under energy stress to support synaptic function. *Neuron* **90**, 278–291 (2016).
15. S. Mazurek, F. Hugo, K. Failing, E. Eigenbrodt, Studies on associations of glycolytic and glutaminolytic enzymes in MCF-7 cells: Role of P36. *J. Cell. Physiol.* **167**, 238–250 (1996).
16. D. Rakus, P. Mamczur, A. Gizak, D. Dus, A. Dzugaj, Colocalization of muscle FBPase and muscle aldolase on both sides of the Z-line. *Biochem. Biophys. Res. Commun.* **311**, 294–299 (2003).
17. M. E. Campanella, H. Chu, P. S. Low, Assembly and regulation of a glycolytic enzyme complex on the human erythrocyte membrane. *Proc. Natl. Acad. Sci. U.S.A.* **102**, 2402–2407 (2005).
18. P. Mamczur, D. Dus, A. Dzugaj, Colocalization of aldolase and FBPase in cytoplasm and nucleus of cardiomyocytes. *Cell Biol. Int.* **31**, 1122–1130 (2007).
19. M. E. Campanella *et al.*, Characterization of glycolytic enzyme interactions with murine erythrocyte membranes in wild-type and membrane protein knockout mice. *Blood* **112**, 3900–3906 (2008).
20. C. L. Kohnhorst *et al.*, Identification of a multienzyme complex for glucose metabolism in living cells. *J. Biol. Chem.* **292**, 9191–9203 (2017).
21. Y. Zhu *et al.*, The long noncoding RNA glycoLINC assembles a lower glycolytic metabolon to promote glycolysis. *Mol. Cell* **82**, 542–554.e6 (2022).
22. X. P. Wen *et al.*, Identification of different proteins binding to Na, K-ATPase alpha1 in LPS-induced ARDS cell model by proteomic analysis. *Proteome Sci.* **20**, 10 (2022).
23. C. Wan *et al.*, Panorama of ancient metazoan macromolecular complexes. *Nature* **525**, 339–344 (2015).
24. B. Wang *et al.*, POH1 contributes to hyperactivation of TGF-beta signaling and facilitates hepatocellular carcinoma metastasis through deubiquitinating TGF-beta receptors and caveolin-1. *EBioMedicine* **41**, 320–332 (2019).
25. M. E. Cockman *et al.*, Lack of activity of recombinant HIF prolyl hydroxylases (PHDs) on reported non-HIF substrates. *Elife* **8**, e46490 (2019).
26. M. J. Strowitzki, E. P. Cummins, C. T. Taylor, Protein hydroxylation by hypoxia-inducible factor (HIF) hydroxylases: Unique or ubiquitous? *Cells* **8**, 384 (2019).
27. G. L. Semenza, P. H. Roth, H. M. Fang, G. L. Wang, Transcriptional regulation of genes encoding glycolytic enzymes by hypoxia-inducible factor 1. *J. Biol. Chem.* **269**, 23757–23763 (1994).
28. J. W. Kim, I. Tchernyshyov, G. L. Semenza, C. V. Dang, HIF-1-mediated expression of pyruvate dehydrogenase kinase: A metabolic switch required for cellular adaptation to hypoxia. *Cell Metab.* **3**, 177–185 (2006).
29. I. Papandreou, R. A. Cairns, L. Fontana, A. L. Lim, N. C. Denko, HIF-1 mediates adaptation to hypoxia by actively downregulating mitochondrial oxygen consumption. *Cell Metab.* **3**, 187–197 (2006).
30. B. I. Kurganov, N. P. Sugrobova, L. S. Mil'man, Supramolecular organization of glycolytic enzymes. *J. Theor. Biol.* **116**, 509–526 (1985).
31. T. N. Seagroves *et al.*, Transcription factor HIF-1 is a necessary mediator of the pasteur effect in mammalian cells. *Mol. Cell. Biol.* **21**, 3436–3444 (2001).

32. J. C. Villa *et al.*, Nontranscriptional role of Hif-1alpha in activation of gamma-secretase and notch signaling in breast cancer. *Cell Rep.* **8**, 1077–1092 (2014).
33. M. E. Hubbi *et al.*, A nontranscriptional role for HIF-1alpha as a direct inhibitor of DNA replication. *Sci. Signal.* **6**, ra10 (2013).
34. J. W. Lee *et al.*, Transcription-independent induction of ERBB1 through hypoxia-inducible factor 2A provides cardioprotection during ischemia and reperfusion. *Anesthesiology* **132**, 763–780 (2020).
35. H. Troy *et al.*, Metabolic profiling of hypoxia-inducible factor-1**β**-deficient and wild type Hepa-1 cells: Effects of hypoxia measured by 1H magnetic resonance spectroscopy. *Metabolomics* **1**, 293–303 (2005).
36. J. R. Griffiths *et al.*, Metabolic changes detected by in vivo magnetic resonance studies of HEPA-1 wild-type tumors and tumors deficient in hypoxia-inducible factor-1beta (HIF-1beta): Evidence of an anabolic role for the HIF-1 pathway. *Cancer Res.* **62**, 688–695 (2002).
37. A. T. J. Wierenga *et al.*, HIF1/2-exerted control over glycolytic gene expression is not functionally relevant for glycolysis in human leukemic stem/progenitor cells. *Cancer Metab.* **7**, 11 (2019).
38. M. Castellana *et al.*, Enzyme clustering accelerates processing of intermediates through metabolic channeling. *Nat. Biotechnol.* **32**, 1011–1018 (2014).
39. S. Jang *et al.*, Phosphofructokinase relocalizes into subcellular compartments with liquid-like properties in vivo. *Biophys. J.* **120**, 1170–1186 (2021).
40. F. R. Opperdoes, P. Borst, Localization of nine glycolytic enzymes in a microbody-like organelle in Trypanosoma brucei: The glycosome. *FEBS Lett.* **80**, 360–364 (1977).
41. R. R. Fagundes *et al.*, HIF1alpha-dependent induction of TFRC by a combination of intestinal inflammation and systemic iron deficiency in inflammatory bowel disease. *Front. Physiol.* **13**, 889091 (2022).
42. B. Turriziani *et al.*, On-beads digestion in conjunction with data-dependent mass spectrometry: A shortcut to quantitative and dynamic interaction proteomics. *Biology (Basel)* **3**, 320–332 (2014).
43. J. Rappsilber, M. Mann, Y. Ishihama, Protocol for micro-purification, enrichment, pre-fractionation and storage of peptides for proteomics using StageTips. *Nat. Protoc.* **2**, 1896–1906 (2007).
44. J. Cox, M. Mann, MaxQuant enables high peptide identification rates, individualized p.p.b.-range mass accuracies and proteome-wide protein quantification. *Nat. Biotechnol.* **26**, 1367–1372 (2008).
45. S. Tyanova, T. Temu, J. Cox, The MaxQuant computational platform for mass spectrometry-based shotgun proteomics. *Nat. Protoc.* **11**, 2301–2319 (2016).
46. J. Cox *et al.*, Andromeda: A peptide search engine integrated into the MaxQuant environment. *J. Proteome Res.* **10**, 1794–1805 (2011).
47. J. Cox *et al.*, Accurate proteome-wide label-free quantification by delayed normalization and maximal peptide ratio extraction, termed MaxLFQ. *Mol. Cell Proteomics* **13**, 2513–2526 (2014).
48. S. Tyanova *et al.*, The Perseus computational platform for comprehensive analysis of (prote)omics data. *Nat. Methods* **13**, 731–740 (2016).
49. S. J. Kierans *et al.*, Hypoxia induces a glycolytic complex in intestinal epithelial cells independent of HIF-1-driven glycolytic gene expression Dataset 1. Proteomics Identifications Database. https://www.ebi.ac.uk/pride/archive/projects/PXD036950. Deposited 22 September 2022.
50. S. J. Kierans *et al.*, Hypoxia induces a glycolytic complex in intestinal epithelial cells independent of HIF-1-driven glycolytic gene expression Dataset 2. Proteomics Identifications Database. https://www.ebi.ac.uk/pride/archive/projects/PXD037020. Deposited 27 September 2022.
51. S. J. Kierans *et al.*, Hypoxia induces a glycolytic complex in intestinal epithelial cells independent of HIF-1-driven glycolytic gene expression Dataset 3. Proteomics Identifications Database. https://www.ebi.ac.uk/pride/archive/projects/PXD037115. Deposited 30 September 2022.